National Research Council Canada
Conseil national de recherches Canada

Institute for Research in Construction
Institut de recherche en construction

Analysis of Simultaneous Heat and Moisture Transport Through Glass Fibre Insulation

by M.K. Kumaran and G.P. Mitalas

Reprinted from
Heat Transfer in Buildings and Structures
HTD Vol. 78, Book No. HOO397
1987 National Heat Transfer Conference, ASME/AICHE
Pittsburgh, PA, August 9 - 12, 1987
p. 1 - 6
(IRC Paper No. 1492)

Price $3.00

NRCC 28488

Canada

RÉSUMÉ

Les auteurs présentent un modèle mathématique basé sur des expressions empiriques des flux de chaleur et d'humidité et servant à décrire le transport simultané de chaleur et d'humidité dans l'isolant de fibre de verre. Ils utilisent ensuite la méthode des différences finies pour analyser les processus de transport. Certaines des prévisions établies lors de l'analyse sont comparées aux mesures en laboratoire.

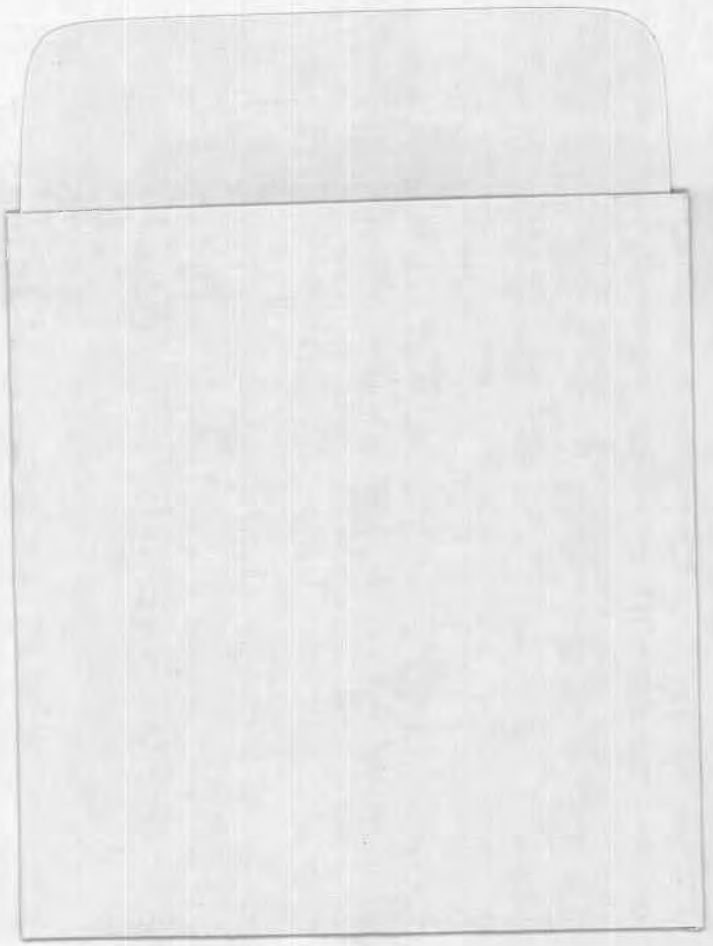

ANALYSIS OF SIMULTANEOUS HEAT AND MOISTURE TRANSPORT THROUGH GLASS FIBRE INSULATION

M. K. Kumaran and G. P. Mitalas
Institute for Research in Construction
National Research Council Canada
Ottawa, Ontario, Canada

ABSTRACT

A mathematical model based on empirical expressions for heat and moisture fluxes is presented to describe simultaneous heat and moisture transport through glass fibre insulation. A finite difference method is subsequently used to analyse the transport processes. Some of the predictions from the analysis are compared with laboratory measurements.

NOMENCLATURE

C = heat capacity of water
H = enthalpy of water
ΔH = enthalpy of vapourisation
I = rate of generation
j = number of slices
J = flux
K(T) = apparent thermal conductivity
K = empirical coefficients
m = mass of moisture
p = water vapour pressure
q = quantity of heat
Q = measured heat flux
t = time
T = temperature
υ = volume element
x = distance

Subscripts
C = cold surface
H = hot surface
m = moisture
q = heat
β = entity transported

INTRODUCTION

Heat and mass transport processes are conventionally described using mathematical models based on conservation principles. For a control volume υ in the medium through which any entity β is transported, the conservation of β in υ at any instant t is written as [1],

Rate of storage of β in υ	=	Rate of entry of β into υ through all the bounding surfaces	+	Rate of generation of β in υ	(1)

or symbolically,

$$\frac{d\beta}{dt} = \text{div } J_\beta + I_\beta \qquad (2)$$

where J_β is the flux of β and I_β is the rate of generation of β. For a one dimensional transport process in the direction x, at any point in the medium, equation (2) reduces to

$$\frac{d\beta}{dt} = \frac{d}{dx} J_\beta + I_\beta \qquad (3)$$

A major practical difficulty in the application of equation (3) is to define J_β unambiguously. Traditionally, well known phenomenological laws such as Fourier's law, Fick's law and Darcy's law are used to define J_β. But that leads to the formidable task of determining the dependence of the transport coefficients on the driving potentials defined by the phenomenological laws. A survey of literature on simultaneous heat and moisture transport shows that very little information exists on the above transport coefficients of building materials that are currently used. This paper describes a method that overcomes the above difficulty and analyses simultaneous heat and moisture transport through glass fibre insulation, one of the most commonly used thermal insulations in buildings.

It was recently shown [2] that for a specimen of glass fibre insulation, for a range of experimental conditions that represent practical building situations, the moisture flux J_m in the presence of a thermal gradient dT/dx is well represented by the empirical expression

$$J_m = K_1 \frac{dp}{dx} + K_2 \frac{dT}{dx} \qquad (4)$$

where dp/dx is the vapour pressure gradient that corresponds to dT/dx and K_1 and K_2 are two material characteristics. For similar experimental conditions as above, it is also well established that the heat flux J_q through a dry thermal insulation is represented by the empirical expression

$$J_q = K(T) \frac{dT}{dx} \tag{5}$$

where the apparent thermal conductivity K(T), at any temperature T is given by

$$K(T) = K_3 + K_4 T \tag{6}$$

and K_3 and K_4 are again two material characteristics. Empirical relations such as (4) and (6) unambiguously define fluxes in equation (3) for the range of experimental conditions selected and lead to the following mathematical model for simultaneous heat and moisture transport through glass fibre insulation.

THE MATHEMATICAL MODEL

From equations (3) and (4), the conservation equation for the moisture transfer is

$$\frac{dm}{dt} = \frac{d}{dx} \left(K_1 \frac{dp}{dx} + K_2 \frac{dT}{dx}\right) + I_m \tag{7}$$

where m is the mass of moisture and I_m is the rate of generation of moisture. All the materials chosen for the present investigation are non-hygroscopic and hence I_m is assumed to be negligible.

Similarly, from equations (3), (5) and (6), the conservation equation for heat transfer is

$$\frac{dq}{dt} = \frac{d}{dx} (K_3 + K_4 T) \frac{dT}{dx} + I_q \tag{8}$$

where q is the quantity of heat and I_q is the rate of heat generated. It was shown [2] that during the process selected for the present investigation, water is transported through the medium, under the influence of a temperature gradient, predominantly by vaporization at higher temperature, vapour diffusion and subsequent condensation at lower temperature. Hence I_q in equation (8) is given by

$$I_q = \frac{dm}{dt} \cdot \Delta H + J_m \cdot C \cdot \frac{dT}{dx} \tag{9}$$

where ΔH is the enthalpy of vaporization and C is the heat capacity of water.

MATERIALS, EXPERIMENTAL METHOD AND RESULTS

The following four specimens of glass fibre insulation were used for the experimental investigations:

Specimen I: 58.8 cm × 58.5 cm slab with 5.5 cm thickness and a bulk density of 30 $kg \cdot m^{-3}$

Specimen II: 58.5 cm × 58.5 cm slab with 5.1 cm thickness and a bulk density of 66 $kg \cdot m^{-3}$

Specimen III: 58.0 cm × 58.1 cm slab with 5.5 cm thickness and a bulk density of 117 $kg \cdot m^{-3}$

Specimen IV: Six 58.0 cm × 58.0 cm slices that form a slab of thickness 15.4 cm with a bulk density of 45 $kg \cdot m^{-3}$

A 60 cm × 60 cm heat flow meter apparatus was used to monitor the heat flux as a function of time for the heat and moisture transport process represented by Figure 1. Measurements were done on all the four specimens at five or six pairs of hot surface temperature T_H and cold surface temperature T_C. The details of the experimental measurements have been reported earlier [2].*

The heat flux for the process represented by Figure 1 showed the general characteristic as in Figure 2; the region BC was always a well defined initial steady state, followed by the transient state similar to the region CD and the system then established the well defined final steady state DE. The processes that occur in the above three regions have been identified [2] as follows:

BC - simultaneous heat and moisture transport at a steady rate,
CD - moisture being progressively vanished from hot to cold surface, and
DE - heat transport at a steady rate.

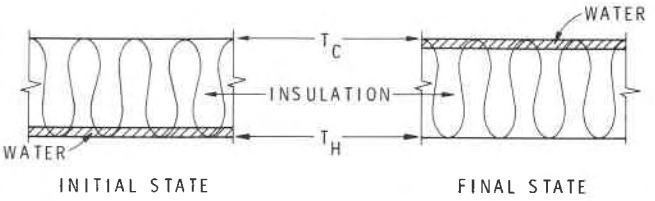

Fig. 1 Schematic representation of the simultaneous heat and moisture transfer investigated; T_H is the hot surface temperature and T_C is the cold surface temperature. The thickness of the water layer is approximately 0.25 mm.

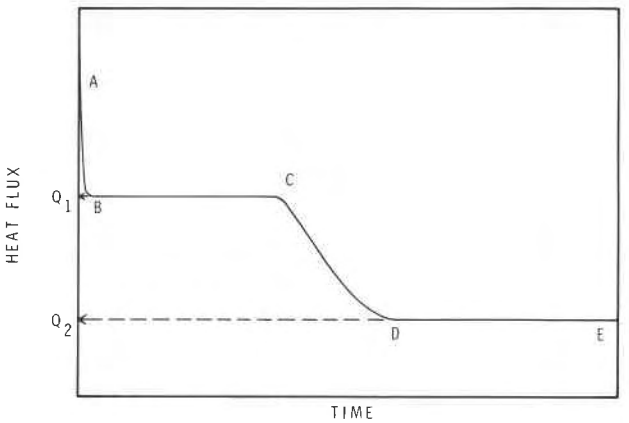

Fig. 2 History of average heat flux during the process represented by Figure 1; Q_1 and Q_2 are the heat fluxes during the initial and final steady states, respectively.

*For specimen IV the temperature at each of the interfaces of the six layers was also monitored during the transport process.

TABLE 1. Experimental data on the four specimens; T_H is the hot surface temperature, T_C is the cold surface temperature, Q_1 and Q_2 are heat fluxes at initial and final steady states and ρ is the density of the specimen.

Specimen	T_H/°C	T_C/°C	Q_1/W•m^{-2}	Q_2/W•m^{-2}
	34.72	13.75	39.6	13.9
Specimen I	39.75	13.94	53.8	17.4
	44.18	14.15	67.9	20.6
ρ = 30 kg•m^{-3}	48.67	14.36	84.2	23.7
	53.09	14.55	102.8	27.0
	30.65	13.55	30.7	11.1
Specimen II	34.61	13.69	39.6	13.6
	37.45	13.85	47.6	15.4
ρ = 66 kg•m^{-3}	40.19	14.04	55.4	17.3
	42.82	14.10	63.4	18.9
	45.33	14.18	72.7	21.0
	36.06	12.17	41.8	15.4
Specimen III	39.10	12.24	49.9	17.4
	41.88	12.34	57.4	19.1
ρ = 117 kg•m^{-3}	44.73	12.48	67.4	21.1
	47.45	12.58	76.8	22.8
	50.27	12.71	87.3	24.6
	36.38	11.69	17.9	5.9
Specimen IV*	40.85	11.80	23.3	7.1
	45.56	11.82	29.9	8.6
ρ = 45 kg•m^{-3}	50.04	11.85	37.2	9.6
	53.41	11.90	43.9	10.4

*The amount of moisture used with specimen IV varied from 150 g to 75 g whereas with the other three specimens it was approximately 100 g.

The experimental results on all the four specimens are summarized in Table 1. The results were analysed, in terms of the thermodynamic model reported earlier [2], to arrive at the material characteristics K_1 and K_2 in equation (4) for each of the specimens. The above model assumes that the moisture transport through the specimens is represented by the thermodynamic process,

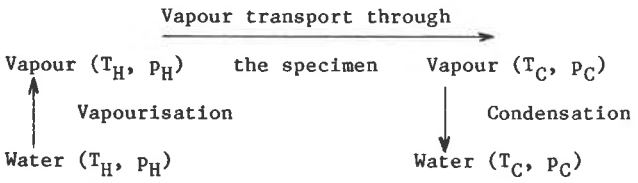

where T_H and T_C are the hot and cold surface temperatures of the specimen and p_H and p_C are the corresponding saturated water vapour pressures. Thus the moisture flux, J_m, in equation (4) is exclusively water vapour flux and is calculated for each pair of T_H and T_C from the thermodynamic relation

$$J_m = (Q_1 - Q_2)/(\Delta H + (H_H - H_C))$$

Where Q_1 and Q_2 are respectively the heat fluxes in the regions BC and DE in Figure 2, ΔH is the average enthalpy of vapourisation for the temperature range T_H to T_C, and H_H and H_C are the enthalpy of water at T_H and T_C, respectively. The constants K_1 and K_2 for the specimens, calculated from a subsequent least-squares analysis, are given in Table 2; the constants K_3 and K_4 in equation (6) were determined by a linear least-squares analysis of the apparent thermal conductivities of each of the dry specimens at various mean temperatures and also are given in Table 2.

SOLUTION OF THE CONSERVATION EQUATIONS

For the mathematical analysis of simultaneous heat and moisture transport through the test specimens, the conservation equations (7) and (8) are solved numerically as outlined in Appendix A. The specimen is treated as formed by a number j of slices of thickness Δx each. Equations (7) and (8) are then written for the finite increment Δx in thickness and for a finite increment Δt in time. It was found that a combination of Δx = 2 mm and Δt = 10 s and of Δx = 5 mm and Δt = 10 s were suitable for all the calculations done on specimens I to III and specimen IV respectively - suitable in terms of computer time as well as desired precision of the calculated results.

DISCUSSION

The finite difference method outlined in Appendix A was used to calculate the data shown in Figures 3a and 4a. The corresponding experimental data are plotted in Figures 3b and 4b, respectively. Except for the sharp break in the heat flux curves at the completion of the initial steady state, the sets of curves in Figures 3a and 3b are practically identical; the heat fluxes at the initial steady states, the duration of the initial steady states and the duration of the transient state between the initial and final steady states are well reproduced. The smooth experimental curves suggest that the non-hygroscopic nature of the material, assumed for the calculations is an approximation. It is to be expected that real materials, depending on their ability to retain moisture will deviate from the behaviour calculated according to the model presented in this paper.

The above calculations were repeated for all the test specimens for all the boundary conditions chosen

TABLE 2. The material characteristics K_1, K_2, K_3 and K_4, given by equations (4) and (6), for the four specimens.

Specimen	K_1/g•m^{-1}•s^{-1}•Pa^{-1} experimental	K_1/g•m^{-1}•s^{-1}•Pa^{-1} adjusted	K_2/g•m^{-1}•s^{-1}•K^{-1}	K_3/W•m^{-1}•K^{-1}	K_4/W•m^{-1}•K^{-2}
Specimen I	1.17×10^{-7}	1.23×10^{-7}	4.21×10^{-6}	-1.450×10^{-2}	1.70×10^{-4}
Specimen II	1.05×10^{-7}	1.13×10^{-7}	5.58×10^{-6}	2.162×10^{-3}	1.01×10^{-4}
Specimen III	1.15×10^{-7}	1.18×10^{-7}	2.17×10^{-6}	9.903×10^{-3}	8.6×10^{-5}
Specimen IV	1.44×10^{-7}	1.54×10^{-7}	1.68×10^{-6}	-7.546×10^{-3}	1.48×10^{-4}

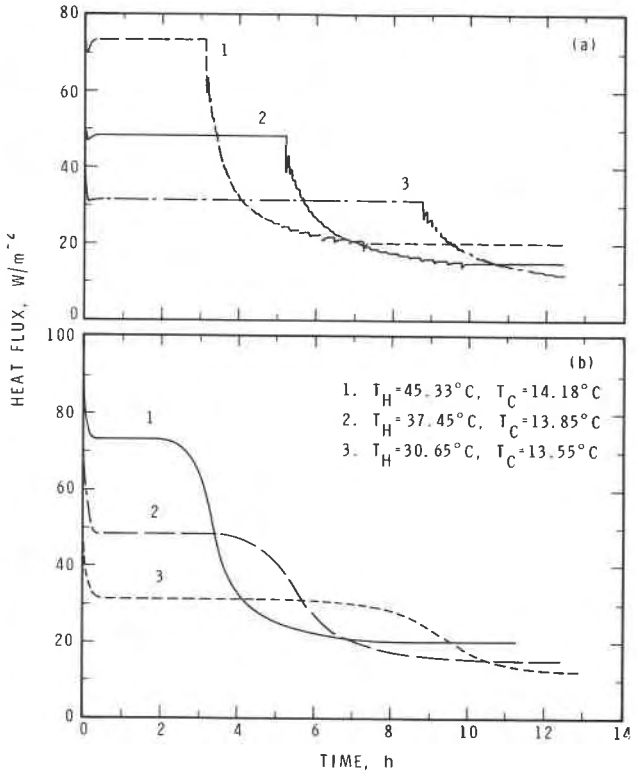

Fig. 3 History of heat flux through Specimen II for three different boundary conditions
(a) calculated using the finite difference method
(b) experimental results

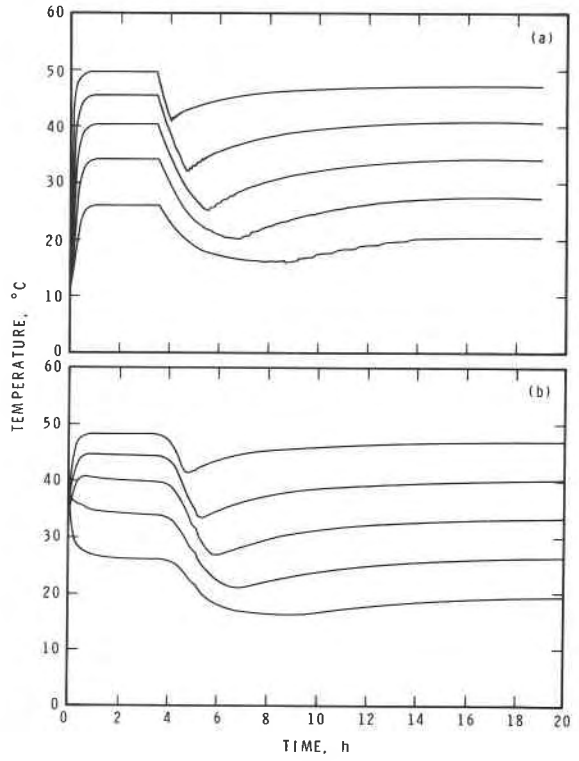

Fig. 4 Variation of temperature at different locations in Specimen IV for boundary conditions, T_H = 53.41°C and T_C = 11.90°C
(a) calculated using the finite difference method
(b) experimental results

for the experiments. The calculated values of the heat fluxes at the initial steady states and the deviations from the experimental values are given in Table 3. The final steady states correspond to heat transfer through dry material and are exactly represented by the model by using only the thermal conductivities given by equation (6).

The magnitude of the heat fluxes is very sensitive to the value of K_1 in equation (4); the experimental values for K_1 derived by the method described in reference [2] and were adjusted, within the limits of the uncertainty determined by the initial least-squares analysis [2], to arrive at best values to represent the behaviour of each specimen for the range of experimental conditions chosen. The adjusted values are given in Table 2. Table 3 shows that one set of material characteristics K_1, K_2, K_3 and K_4, independent of the boundary conditions and driving forces, describes the simultaneous heat and moisture transport through each test specimen.

Comparison of Figures 4a and 4b adds further confidence on the method described in this paper. To generate the curves in Figure 4a only the boundary conditions and the material characteristics were used. The variation of temperature during the simultaneous heat and moisture transport, at different locations within the slab, is well predicted by the method as is demonstrated by the experimentally generated curves in Figure 4b, in all their details, particularly the drop in temperature at the completion of the steady state followed by an increase in temperature as the movement of moisture stops at that location. The instant at which this reversal of temperature change occurs at different locations within the slab are also well predicted by the model.

CONCLUSIONS

In practical building situations within the limits of the boundary conditions chosen for the experiments, the simultaneous heat and moisture transport through non-hygroscopic glass fibre insulation can be predicted using four material properties. These properties are independent of the boundary conditions and the distribution of moisture. This is an advantage over the traditional method where the concept of "effective thermal conductivity" of moist thermal insulations is used. The above quantity is not a material property in the sense that it depends on the boundary conditions as well as on the moisture distribution.

The calculations used to generate the data on temperature, shown in Figure 4a, could be used to generate parallel data on vapour pressure and moisture content at various locations. Further experimental investigations are desirable to check the applicability of the present approach.

The approach discussed in this paper provides a basis for further research on heat and moisture transport through hygroscopic building materials. Appropriate empirical expressions will have to be

TABLE 3. The heat flux Q_1 during the initial steady states as calculated using the finite difference method; T_H the hot surface temperature and T_C the cold surface temperature are in the same order as in Table 1; ΔQ is the difference Q_1 (measured) - Q_1 (calculated).

Specimen	$Q_1(W \cdot m^{-2})$	$\Delta Q(W \cdot m^{-2})$
	39.3	0.3
	39.6	0.0
Specimen I	53.3	0.5
	67.5	0.4
	84.2	0.0
	103.5	-0.7
	30.9	-0.2
	40.3	-0.6
Specimen II	47.8	-0.2
	55.6	-0.2
	64.0	-0.6
	72.7	0.0
	41.8	0.0
	49.7	0.1
Specimen III	57.6	-0.2
	66.6	0.7
	76.0	0.8
	86.7	0.7
	18.0	-0.1
	23.2	0.1
Specimen IV	29.7	0.2
	37.1	0.1
	43.5	0.4

developed to define the moisture generation term that appears in the moisture conservation equation.

ACKNOWLEDGMENT

The authors gratefully acknowledge the technical assistance of Mr. R.G. Marchand for this work. This paper is a contribution of the Institute for Research in Construction, National Research Council of Canada.

REFERENCES

1. Mikhailov, M.D. and Osizik, M.N. Unified analysis and solutions of heat and mass diffusion, John Wiley & Sons, New York, 1984, p. 2.

2. Kumaran, M.K. "Moisture transport through glass-fibre insulation in the presence of a thermal gradient", Journal of Thermal Insulation, in press.

APPENDIX A NUMERICAL SOLUTION OF THE CONSERVATION EQUATIONS

The conservation equations (7) and (8) can be approximated by a set of finite difference equations in terms of increments Δx and Δt in thickness and time respectively. Thus at a given instant t, temperatures, vapour pressures, heat and moisture fluxes and heat and moisture storages can be related by the matrix equations,

$$|B| \cdot |T| = |I| \qquad (10)$$

and

$$|C| \cdot |P| + |D| \cdot |T| = |G| \qquad (11)$$

where $|T|$, $|P|$, $|I|$ and $|G|$ are column matrices with J-1 elements and $|B|$, $|C|$ and $|D|$ are square matrices of J-1th order,

J = $L/\Delta x$, the number of slices that makes up the specimen with J-1 interfaces between the slices.

L = specimen thickness

Δx = slice thickness.

The elements of the matrices are the following:

T_j = temperature at the interface of slices j and j+1

P_j = vapour pressure at the above interface, calculated from the equation*

$$P_j = (22.565 - 2377.1/T_j - 33623/T_j^{1.5}) \qquad (12)$$

$$B_{j,j} = -(b_j + b_{j+1}),$$

$$B_{j,j-1} = b_j \text{ and}$$

$$B_{j,j+1} = b_{j+1}$$

where,

b_j = thermal conductance of slice j calculated using equation (6).

All other elements of $|B| = 0$

$$C_{j,j} = -2K_1$$

$$C_{j,j-1} = C_{j,j+1} = K_1$$

$$D_{j,j} = -2K_2$$

*equation valid for the range $273.15K \leq Tj \leq 330K$

$$D_{j,j-1} = D_{j,j+1} = K_2,$$

where K_1 and K_2 are the material characteristics defined by equation (4).

All other elements in $|C|$ and $|D|$ are also equal to zero.

$G_j = \Delta M_j$, except G_1 and G_{J-1}

ΔM_j = Change in moisture flow at the interface of slices j and j+1

The boundary conditions are defined by the hot and cold surface temperatures T_H and T_C and the corresponding vapour pressures P_H and P_C and hence G_j at the first and last interfaces become

$$G_1 = \Delta M_1 - (K_1 P_H + K_2 T_H) \tag{13}$$

and

$$G_{J-1} = \Delta M_{J-1} - (K_1 P_C + K_2 T_C) \tag{14}$$

I_j the change in the heat flow at the interface of slices j and j+1 is defined by

$$I_j = I_{1j} + I_{2j} + I_{3j} \tag{15}$$

except I_1 and I_{J-1} which incorporate boundary temperatures as

$$I_1 = I_{11} + I_{21} + I_{31} - T_H b_1 \text{ and} \tag{16}$$

$$I_{J-1} = I_{1J-1} + I_{3J-1} - T_C b_J, \tag{17}$$

where

$$I_{1j} = \Delta M_j \cdot \Delta H_j$$

and ΔH_j is the enthalpy of vapourization at T_j, calculated by differentiating equation (12) with respect to temperature and substituting for the derivative dp/dT in Clausius-Clapeyron equation for water to water vapour transition. I_{2j} is the change in heat stored in water and the slice at j defined as

$$I_{2j} = (T'_j - T_j) \cdot (M_{1j} \cdot C_m + \omega \cdot C_o) \tag{18}$$

where T'_j is the temperature at time $t - \Delta t$, M_{1j} is the moisture stored at j, ω is the mass of the slice of insulation, C_m is the specific heat of water and C_o that of the insulation. The quantity I_{3j} is the change in the amount of heat carried by water vapour that flows through the specimen and is defined as

$$I_{3j} = \frac{C_v}{2}\left((T_{j-1} - T_j) \cdot M_j + (T_j - T_{j-1}) \cdot M_{j+1}\right) \tag{19}$$

where C_v is the specific heat of water vapour and M_j is the water vapour flow calculated according to equation (4) as

$$M_j = K_1 (P_{j-1} - P_j) + K_2 (T_{j-1} - T_j) \tag{20}$$

At any instant and at any interface, saturation conditions may or may not exist. If liquid water is present (i.e. $M_j \neq 0$) or if temperature and vapour pressure conditions are such that water vapour condenses, then saturation conditions exist and it is assumed that at such locations equation (12) is valid. Otherwise, for the sake of consistency, equation (4) is assumed to be valid even at vapour pressures lower than saturation vapour pressures and P_j is calculated with G_j set equal to zero (i.e., no evaporation or condensation). In doing so, a situation analogous to the thermal diffusion of a gas is considered. Calculations show that, at locations where saturation conditions do not exist, maintaining vapour pressure equal to P_C has insignificant effect on the results.

The solution of the above equations is achieved by two sets of iterative procedures, one operating within the other. The mathematical technique also utilizes a matrix inversion procedure. The main iterative procedure calculates $|B|$ from $|T|$ and it incorporates the second iterative procedure that calculates $|T|$ and $|P|$ at time t for a given $|B|$. For the latter set of iterations, the temperature T_{nj} for the n^{th} cycle is updated by

$$T_{nj} = T'_j + F.(T_j - T'_j) \tag{21}$$

where

T_j = temperature calculated at the latest stage of iteration,
T'_j = temperature calculated at the previous stage and
$F < 1.0$.

The present calculations indicate that F = 0.1, in most cases, gives a stable and rapid convergence. These iterative calculations are terminated when ER > 0.01

where

$$ER = \sum_{j=1}^{j=J-1} |T_j^1 - T_j| \tag{22}$$

The relatively low value of ER used in the present calculations did not significantly affect the computation time.

The purpose of the main iterative procedure is to update the $|B|$. This had to be repeated only three times because for the range of temperature selected for the present investigation, the thermal conductances, b's, are only weak functions of temperature.

The initial and boundary conditions imposed for the experiments are approximated for the calculations as follows. The temperatures at all the interfaces are set equal to T_C, the cold surface temperature, the vapour pressures are set equal to P_C, the saturation vapour pressure at T_C and the moisture storage everywhere is set equal to zero. Then at t = 0, the temperature, vapour pressure and the moisture storage at interface 1 are set equal to T_H, the hot surface temperature, P_H, the corresponding saturated vapour pressure and the total amount of moisture introduced into the specimen. The cold surface temperature, T_C and the corresponding saturated water vapour pressure, P_C, are maintained constant at all times.

reprinted from

Heat Transfer in Buildings and Structures — HTD-Vol. 78
Editors: T.H. Kuehn, and C.E. Hickox
(Book No. H00397)

published by

THE AMERICAN SOCIETY OF MECHANICAL ENGINEERS
345 East 47th Street, New York, N.Y. 10017
Printed in U.S.A.